Investigation Of Electrical And Magnatical Multiples Contributions To The Total Longitudinal And Transvers Firm Factors In Some Positive 25mg States Using Different Interactions

Nabeel F. Lattoofi, Samaher Th.Mashaan
Department of Physics, College of Science, University of Anbar, Iraq

A R T I C L E   I N F O

A B S T R A C T

The nuclear structure of the 25Mg nucleus was studied using the shell model and Skyrme computations. For positive parity low (energy states, inelastic electron scattering form factors, energy levels, charge density distribution, and transition probabilities) have all been determined. The SKX parameters were used with the *sd* shell model. The best results were obtained from HBUMSD, HBUSD, CWH, PW, and W interactions, which were calculated on sd space interactions. For positive parity states, the excitation energies and transition probabilities to the ground state $5/2^+$ have also been determined. The experimental data was compared to the estimated form factors, energy level diagrams, and transition probabilities. The Skyrme interaction was shown to be compatible with a shell model is used to explore nuclear structure.

1.Introdcation

Interest in the wide range of physical events underpins many studies, such as those presented here, that are currently focusing on odd-A magnesium isotopes, with the 25Mg one of the most important Mg nuclides is the nucleus, particularly in astrophysics. The slow-neutron-capture (s) mechanism, a major source of neutrons in the reaction 22Ne (α,n) 25Mg, has been studied in a number of articles. This reaction plays an important role during the combustion of primary helium, in the combustion of the carbon shell [1, 2] , It is an active Mg-Al cycle in H-shell starburst burning[3]. A number of theoretical methods have recently been used to investigate the nuclear structure of this isotope, all of which deal with the hyperonin p orbit. [4, 5] .

The effective interaction between two bodies is a critical component of the nuclear shell model's success, since it dictates the accuracy of calculations that assume an inert core and a finite amount of space (suitable computing methods and the so-called model space). Using quantum-mechanical many-body theory and the realistic nucleon-nucleon (NN) interaction as a starting point Microscopically, the effective interaction is employed to comprehend nuclear properties. The earliest estimates based on shell models[6] between nucleons, they employed Despite 50 years of investigation, a simple square well possibility exists. Has resulted in improved interactions. The existing shell-model algorithms demand that Single-particle energies (SPEs) and two-body matrix elements can be used to create an interaction (TBMEs).

Many shell-model algorithms, such as OXBASH, have been developed to overcome the eigenvalue problem in shell-model calculations.[7], ANTOINE [8], NUSHELL. It was discovered that the effects of core polarization (CP) on the nuclear form factor are essential. for improving computations and comparing with experimental results [9, 10]. Although there is no visible differentiation in the experimental data between the various estimations for the spinning current,, the results for the energy levels investigated show good general agreement.

The first component of the research involves utilizing the shell-model algorithm OXBASH for Windows to find the energy levels and probability current density for a variety various of two-body effective interactions. The HBUMSD,HBUSD,CWH,PW, and W interactions the shell-model algorithms are used sd-shell nuclei to calculate longitudinal and transverse electron scattering form factors for nuclei 25Mg.

The aim of this research is to compute the electron scattering form factor by taking into account the model space and the particle-hole excitation in the core. We also use the aforementioned five effective interactions to compare the energy levels, based on experimental results and theoretical results, and B (E2).

The electron-nucleus scattering form factors for the 25Mg nucleus are calculated using the USDA Hamiltonian's one-body density-matrix elements. For all states in the first sequence, the longitudinal form factor calculations demonstrate strong agreement, however the shell-model predictions for the excitation states in the second sequence indicate a difference in findings. The Woods-Saxon, Skyrme(Sk42), harmonic-oscillator potentials The wave

---

* Corresponding author at: Department of Physics, College of Science, University of Anbar, Iraq
dr.nabeel.fawzi@uoanbar.edu.iq

functions of radial single-particle matrix elements were calculated using these techniques. When utilizing the Sk42 potential, the results of the inelastic transverse form factors correspond well with the experimental data, however the elastic magnetic scattering results reveal a considerable discrepancy in values when compared to the experimental data. When applying the harmonic-oscillator potential, The overall shape and other properties of the form factors, on the other hand, are satisfactory. , by Anwer A. Al-Sammarraie *et al.,*[11].

A shell model and Hartree-Fock computations were used to investigate the elastic and inelastic electron scattering form factors for the 25Mg nucleus. For this nucleus, the USDA two-body effective interaction with the sd shell model space was used to obtain the shell model's wave functions for this nucleus Ali A. Alzubadi *et al.,* on the other hand [12] the Hartree-Fock approach has employed the SkXcsb Skyrme parameterization to obtain the single-particle potential, which is required for the calculation of single-particle matrix elements. The predicted form factors were compared to the experimental data that was available, by G.N. Flaiyh [13] The shell model and Skyrme–Hartree–Fock calculations were used to investigate the nuclear structure of 29-34Mg isotopes at the neutron drip line. For positive low-lying states, Proton, neutron, mass, and charge densities in nuclear physics are computed, together with their accompanying (rms) radii, inelastic electron scattering form factors and neutron skin thicknesses. For the transverse form factor, the inferred results are presented and compared to the experimental data. The ability of the combined the Hartree-Fock mean field with shell model approach with Skyrme interaction to accommodate has been confirmed when exploring diverse nuclear configurations of stable and unstable nuclei, The descriptive and predictive power of nuclear excitation characteristics is quite high. P P Singhal *et al.,* investigated the electron elastic scattering cross-sections of the odd-A nuclei 23Na, 25Mg and 27Al [14] in terms of large-based shell model wave functions in the 1s-0d shell Only if the valence orbits are given a size 6–12 percent less than that required by the root-square radius can magnetic elastic scattering be explained, despite the fact that these wave functions are supposed to appropriately characterize formation mixing. There was no evidence to back up the theory that the orbits of the neutron and proton are different diameters.

The data was used to calculate the M3 and M5 moments. The excited states of ^{25}Mg by E W Lees *et al.,* [15] inelastic electron scattering in the momentum transfer from (0.3 to 1.15 fm-1) has been investigated. Lower transition probabilities and transition radii are observed for seven levels with excitation energies below 4.1 MeV were recorded, and it was discovered that the transition probabilities were more exact than prior observations. In the range of 5-6 MeV excitation energy, researchers looked for hexadecupole strength to the 11/2+ levels. Comparisons

with known electromagnetic strengths, and, more importantly, For the ground state band of 25Mg, an expanded Nilsson-model description was used, were also studied, in relation to the form factors that were measured In the symplectic model,

the electron scattering transverse form factors for the transitions for ^{24}Mg are determined. The sp(3, R) model's predictions outperform computations limited to the valence shell, according to the findings. The consequences of higher shells are not accounted for by simply adding an effective charge factor, as they are in longitudinal form factor calculations, by M.J.Carvalho *et al.,*[16]. The cross sections of elastic electron scattering from the isotopes (^{24}Mg, ^{25}Mg, and ^{26}Mg) have been studied by E.W.Lees *et al.,* [17] in the 0.2 to 1.15 fm-1 momentum transfer range Individual RMS radii, as well as discrepancies between isotopes, are studied. An enhanced Nilsson model calculation is used to compare the measured form factors to the predictions. The inelastic electron cross-sections were calculated and measured from

^{25}Mg is analyzed by J. R. Moreira and J. R. Marinelli [18] at a back angle and in the energy range from 120 to 260 MeV, and tangential form factors results for the two lowest excited levels were extracted from the baseband This new data is compared to spin model calculations, in which the collective current contributions are accounted for in phenomenological and theoretical terms. Although there is no visible differentiation between the different estimates of the rotational current using the data currently available, the general agreement is good for the energy levels investigated.

In the present work, From the factors of the positive parity states in the 25Mg nucleus, we calculate longitudinal, transverse, elastic, and inelastic electron scattering. The *sd* model with SKX parameters was used for the positive parity states consisting of the active *1d$_{5/2}$, 2s$_{1/2}$* and *1d$_{3/2}$* shells above the inactive ^{16}O core in $(1s)^4(1p)^{12}$ which remains closed. The interactions HBUMSD, HBUSD, CWH ,PW and W were used to provide realistic sd-shell wave functions (1d$_{5/2}$, 1d$_{3/2}$, 2s$_{1/2}$) for positive valence states 5/2 $^+$ ground state (GS) 5/2$^+$,1/2 (0.585) MeV, 3/2$^+$ (0.974 MeV), 5/2$^+$ (1.964 MeV), 7/2$^+$ (1.611MeV) , 9/2$^+$ (3.405 MeV) and 11/2$^+$(5.251 MeV) .

2. Theory and methodology

The total form factor can be represents with the electron scattering angle θ as the sum of the two terms; longitudinal $F^L(q)$ and transverse $F^T(q)$ as follows:

$$|F(q)|^2 = |F^L(q)|^2 + [1/2 + \tan^2(\theta/2)][F^T(q)]^2 \qquad (1)$$

For the form factors in the total longitudinal (L) and transverse (T) directions, it can be written as [19]:

$$|F^L(q)|^2 = \sum_{J\geq 0}\left|F^L_J(q)\right|^2 \qquad (2)$$

$$|F^T(q)|^2 = \sum_{J\geq 0}\left\{\left|F^M_J(q)\right|^2 + \left|F^E_J(q)\right|^2\right\} \qquad (3)$$

where $\left|F_J^M(q)\right|^2$ and $\left|F_J^E(q)\right|^2$ is the magnetic transverse form factor, and is the electric transverse form factor, respective.

The sum of the elements of the one-body density matrix's product (OBDM) $X_{J_f}^J J_i\left(t_z, j_i, j_f\right)$ the reduced matrix element of electron scattering was represented by the single-particle matrix elements, operator $\hat{T}_{J,t_z}$ for a chosen model space and is given by [19]:

$$\langle J_f\|\hat{T}_{J,t_z}\|J_i\rangle = \sum_{j,j_f} X_{J_f}^J J_i\left(t_z, j_i, j_f\right)\langle J_f\|\hat{T}_{J,t_z}\|J_i\rangle$$
(4)

with initial and final single-particle states within concerned model space j_f and j_i and $t_z = 1/2$ and $-1/2$ respectively, for proton and neutron.

Center of mass $F_{cm}(q)$ and finite size $F_{fs}(q)$ corrections were included to The momentum transfer q between the initial and final states is involved with the electron scattering form factor, of spin $J_{i,f}$ as follows [20]:

$$\left[F_J^\eta(q)\right]^2$$

$$= \frac{4\pi}{Z^2(2J_I + 1)}\left|\sum_{t_z} e(t_z)\langle J_f\|\hat{T}_{J,t_z}^\eta(q)\|J_I\rangle\right|^2 F_{cm}^2(q) F_{fs}^2(q) \quad (5)$$

with η is either the longitudinal (L), or transverse (T) form factors.

The probability of a decreased transition is given by[21]

$$B(\eta J)$$
$$= \frac{Z^2}{4\pi}\left[\frac{(2J + 1)!!}{k^J}\right]^2 \left[F_J^\eta(k)\right]^2 \quad (6)$$

where k=E$_x$/ ℏc.

$$B(\eta J)J_i = \frac{1^+}{2}$$

$\to J_f$, $B(M1)$ *in units of* u_N^2, $B(E2)$ *in units of* u_N^2 fm^2 , $B(E1)$ *units of* $e^2 fm^2$

The central potential is represented here with the one-body mean field Skyrme potential were used for which is an approximated field provided from all two and three body interactions between nucleons inside the nucleus. This potential can be given in terms of two-and three-body parts as follows [22]:

$$\hat{V}_{Skyrme} = \sum_{i<j} V_{ij}^{(2)} + \sum_{i<j<k} V_{ijk}^{(3)} \quad (7)$$

The two-body section is provided by:

$$\hat{V}^{(2)}{}_{Skyrme} = \hat{V}^m + \hat{V}^{\text{L.S}} + \hat{V}^t$$

$$\hat{V}^m = t_0(1 + x_0\hat{p}_\sigma)\delta_{12} + \frac{t_3}{6}(1 + x_3\hat{p}_\sigma)\rho^\alpha(r_1)\delta_{12} +$$
$$\frac{t_1}{2}(1 + x_1\hat{p}_\sigma)\left(\delta_{12}\hat{k}^2 + \widehat{K}\delta_{12}\right) + (1 + x_2\hat{p}_\sigma)\hat{k}'\hat{k}\delta_{12}$$

$$\hat{V}^{\text{L.S}}$$
$$= it(\hat{\sigma}_1 + \hat{\sigma}_2).\hat{k}'$$
$$* \hat{k}\delta_{12}$$

$$\hat{V}^t = \frac{t_e}{2}\left\{\left(3(\hat{\sigma}_1.\hat{k}')(\hat{\sigma}_2.\hat{k}') - (\hat{\sigma}_1.\hat{\sigma}_2)\hat{k}'^2\right)\delta_{12} + \right.$$
$$\delta_{12}\left(3(\hat{\sigma}_1.\hat{k})(\hat{\sigma}_2.\hat{k}') - (\hat{\sigma}_1.\hat{\sigma}_2)\hat{k}^2\right)\right\} +$$

$$t_0\big(3(\hat{\sigma}_1.\hat{k}')\delta_{12}(\hat{\sigma}_2.\hat{k}') -$$
$$(\hat{\sigma}_1.\hat{\sigma}_2)\hat{k}'.\delta_{12}\hat{k}\big) \quad (8)$$

were $\delta_{12} = \delta(r_1 - r_2)$ and the three-body part by

$$V_{Skyrme}^{(3)} = t_3\delta_{12}\delta_{13} \quad (9)$$

The $\hat{k}$ and $\hat{k}'$ are relative momentum operators, and their definitions are as follows:

$$\hat{k} = \frac{1}{2i}(\vec{\nabla}_1 - \vec{\nabla}_2), \quad \hat{k}' = \frac{1}{2i}\left(\overleftarrow{\vec{\nabla}}_1 - \overleftarrow{\vec{\nabla}}_2\right) \quad (10)$$

with the $\hat{k}'$ acting to the left. The tensor force is usually neglected.

The saturation properties have been presented in the first item of Equ.(8), while surface properties were shown in momentum-dependent terms which is account for finite-range force effect [23]. SkXcsb parameterizations were implemented in this study [24] which delivers the best rms (root-mean-square) results. In the s-wave portion, charge symmetry breaking (CSB) occurs. as well as the normal exchange (CE) factors and Coulomb direct (CD) are included in this parameterization. Folding the computed charge distribution, $P_{ch}(r)$, with the two-body Coulomb interaction yields the direct Coulomb potential, which is given by [25].

$$H_{CD} = \frac{e^2}{2}\iint_0^\infty \frac{\rho_P(r)\rho_P(r^i)}{|r - r^i|} d^3r d^3r^i \quad (11)$$

The first term of the density matrix expansion in the local density approximation is the exchange part of the Coulomb interaction, which derives from the Slater approximation and is given by:

$$H_{CE} = \frac{3e^2}{4}\left(\frac{3}{\pi}\right)^{1/3}\int_0^\infty \rho_P(r)^{4/3} d^3r \quad (12)$$

3. Results and Discussion

The latest version of the OXBASH shell model code uses proton and neutron formalisms have been obtained to calculate the OBDM elements which used then in MJ and EJ matrix elements operators. The single particle elements of radial wave functions were computed using the SHF potentials of the type *SkX* for positive parity states . Since ^{25}Mg has an 12 number of protons, we would expect the proton's contribution to the overall form factor to be forceful for this nucleus. The results will be separated into two parts for discussion. First we introduced we introduced Positive parity states' inelastic electron scattering form factors, energy levels, and transition probabilities arranged according to increasing angular momentum.

The calculations of longitudinal and transverse form factors in positive low parity states case have been adopted using the *sd* model space with different two body effective interactions. Fig.1 shows the inelastic longitudinal C2 form factor for the first $1/2^+$ (0.585 MeV) state using also the five interactions chosen with SKX parameters in the momentum transfer area (0.5 to 1.2 fm-1), gave there is excellent agreement with experimental results. (0.5 to 1.2

fm^{-1}). The calculated curves represented by two peaks are underestimate the experimental data for the region (0.5 to 1.2 fm-1). For the first peak one can see that the calculated result are underestimate the experimental data. The transverse form factors of this transition represented by the sum of the magnetic and electrical form factors for each selected interaction were dissipated in Fig.1 (b). All interactions are in a fine. Fig.1 (c) shows the best interaction with the contribution of the electric curve E2 and the magnetic M3 curve. We notice that the contribution of E2 is less, while the contribution of M3 is large. And that the contribution of electric E2 is consistent at the confined momentum transfer region (1.6 – 3fm^{-1}) with a reasonable contribution at this region, specifically the second peak.
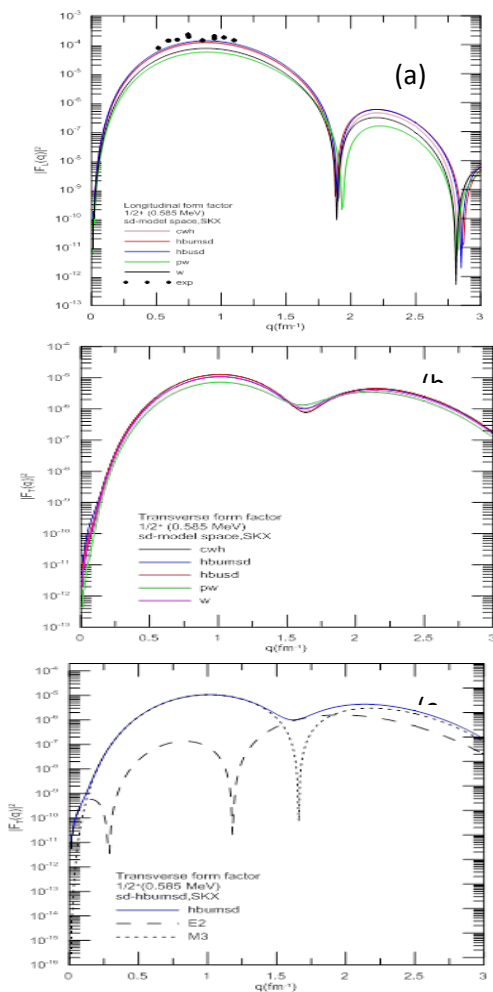
Fig.1 Theoretical 1/2+ longitudinal and transverse form factors (a, b, and c) (0.585 MeV) compared to experimental data using *SkX* parameterization [15].

The computed C2+C4 longitudinal form factors were calculated for first 3/2$^+$ state at 0.974 MeV. An examination of these curves in Fig.2 (a) reveals that the predictions using SKX parameters are in good agreement with the results of the experiments. The longitudinal form factors were calculated for this transition, where the total sum of the

C2+C4 longitudinal form factors agrees well with the experimental data for the five interactions selected for the region where momentum is transferred 0.8 to 1.2 fm^{-1}. In Fig. 2(b) one can notice clearly that the main contribution to the total longitudinal form factors belongs to C2 curve for all momentum transfer, while C4 contribution is considered negligible in all region except for momentum transfer region from (1.5-2fm^{-1}).

Fig.2(c) represents the transverse form factors of the sum of E2+E4 and M1+M3 for the five selected reactions. Fig.2(d) represents the contributions of the total electric and magnetic form factors with the best interaction (HBUMSD). We note that the magnetic curve (M1+M3) has a greater contribution than the electric curve (E2+E4). It is also clear to us that there is a complete agreement of all the transverse form factors (electrical and magnetic) with the total sum in
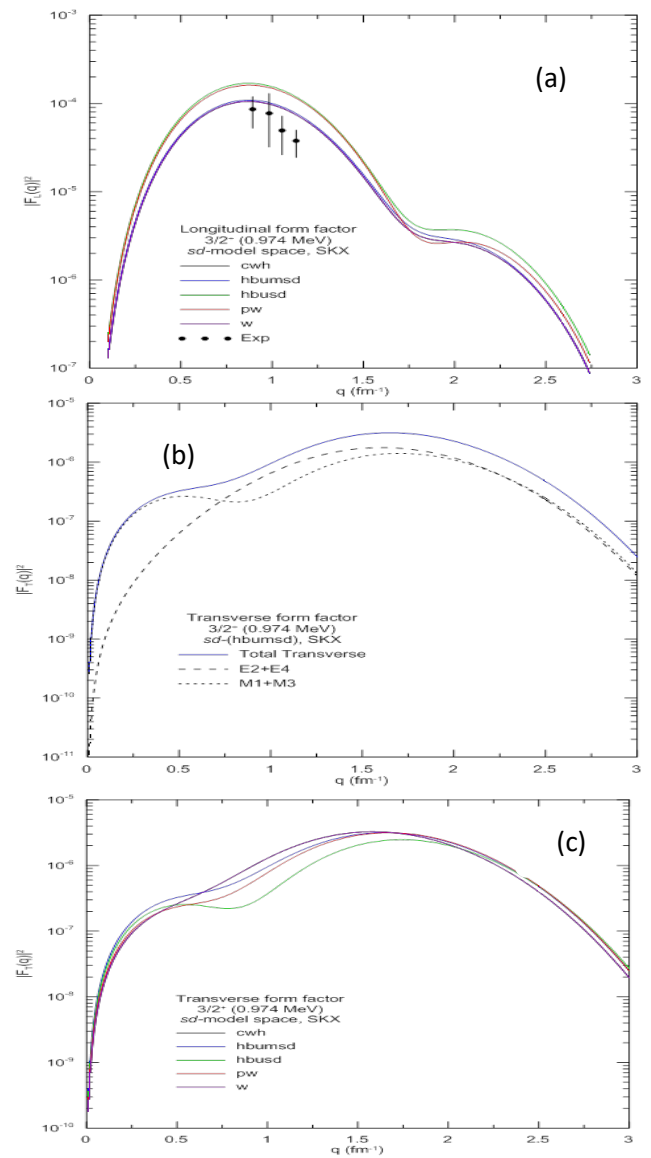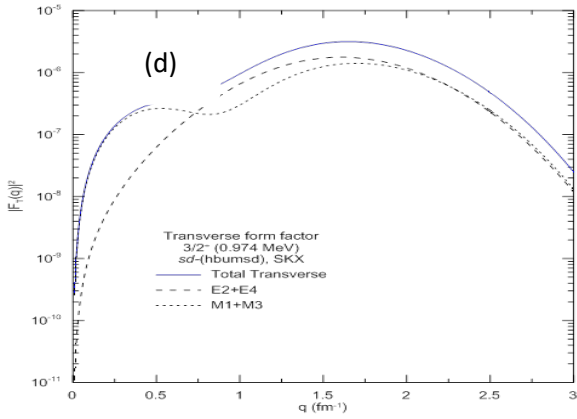

the momentum transfer region greater than 1fm^{-1}.

Fig.2 Longitudinal (a and b) and transverse (c and d) form factors in theory for 3/2+ (0.974MeV) compared to experimental data using SkX parameterization[15].

Fig.3 (a) shows the total inelastic longitudinal form factors (C0+C2 + C4) for the first $5/2^+$ at energy 1.964 MeV computed with *sd* model space using *SKX* parameters for all identified interactions. This figure shows that all interactions are suitable for reproducing the experimental form factor data in the momentum transfer between (0.4 to 2.75 fm^{-1}). The shape of the theoretical curve did not match well with the experimental one for all interactions. As to the longitudinal form factors, the contributions of the Coulomb form factors C2 and C4 to the best HBUMSD interaction extracted from Fig. 3(a) are depicted in Fig. 3(b). We note a small contribution from C0 which is negligible. The contribution of C2 is observed with the experimental data in the momentum transfer region (0.4 to 2.75 fm^{-1}) as in Fig. 3 (a and b)., the total transverse form factors (electrical and magnetic) were shown in Fig.3 (c) for all interactions. Fig.3(d) represents the contribution of the total magnetic (M1+M3+M5) and total electric (E2+E4) form factors using the HBUMSD interaction. One notice that the main contribution belongs to the total magnetic form factors (M1+M3+M5) which shows the largest contribution, we note a small contribution form (E2+E4) is negligible.
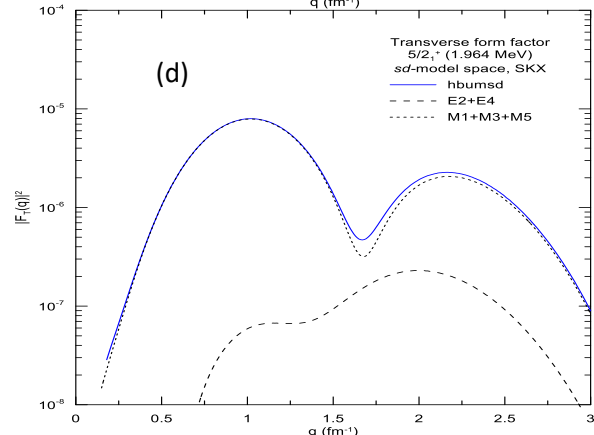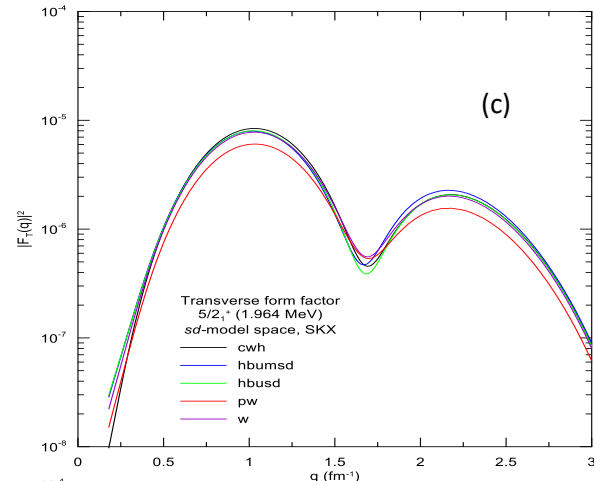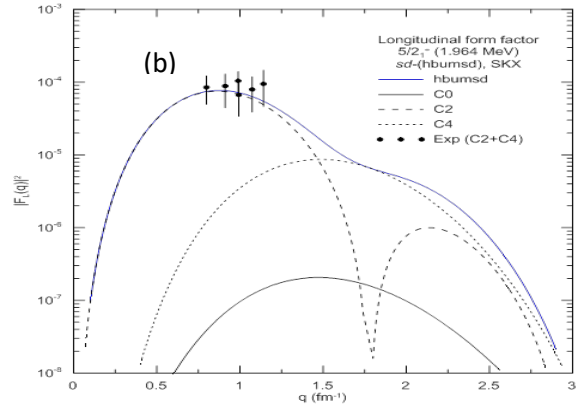

Fig.3 Form factors, theoretical longitudinal (a and b) and transverse (c and d) for 5/2+ (1.964MeV) compared to experimental data using SkX parameterization [15].
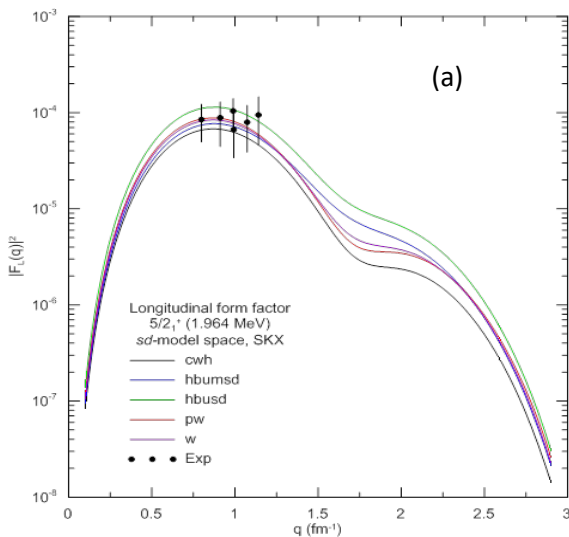
Fig.4 (a) shows C2+C4 inelastic longitudinal form factors for the transition $7/2^+$ (1.611 MeV) for all interactions selected in the momentum transfer between (0.3 to 1.25 fm-1) along with experimental data. The calculated results are in a very good agreement with experimental one for all interactions. Fig.4 (b) represents the best interaction of HBUMSD with the contribution of both C2 and C4 with the experimental data. The contribution of C4 were almost negligible, while the contribution of C2 is greater and can be considered for all momentum transfer region. Fig.4(c) shows the overall transverse form factors that correspond well in the momentum regions. (0.4 to 2.7 fm^{-1}) to the experimental curve is located on top of the theoretical curve. Fig.4(d) represents the best interaction with the

contributions of transverse form factors (electrical and magnetic), as it was noticed that electric (E2+E4) curve gives less contributes to the total transverse form factor in momentum transfer, and the largest contribution is clearly belongs to the magnetic (M1+M3+M5) curve.
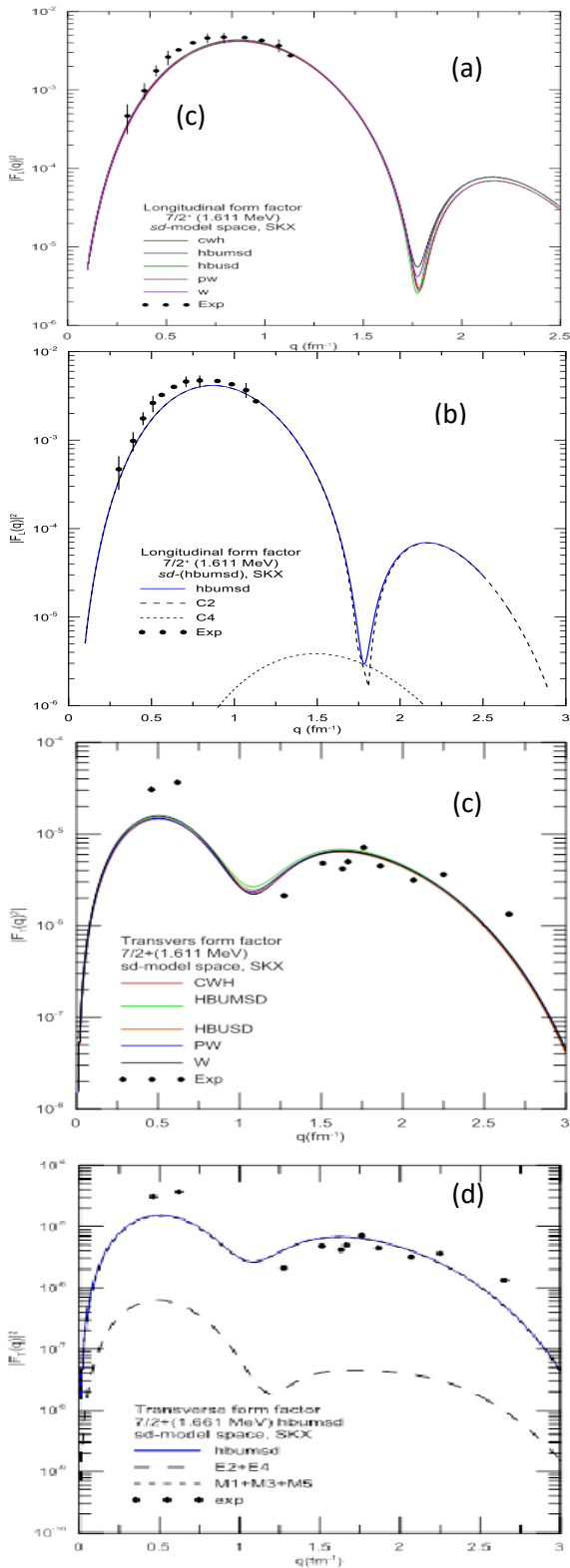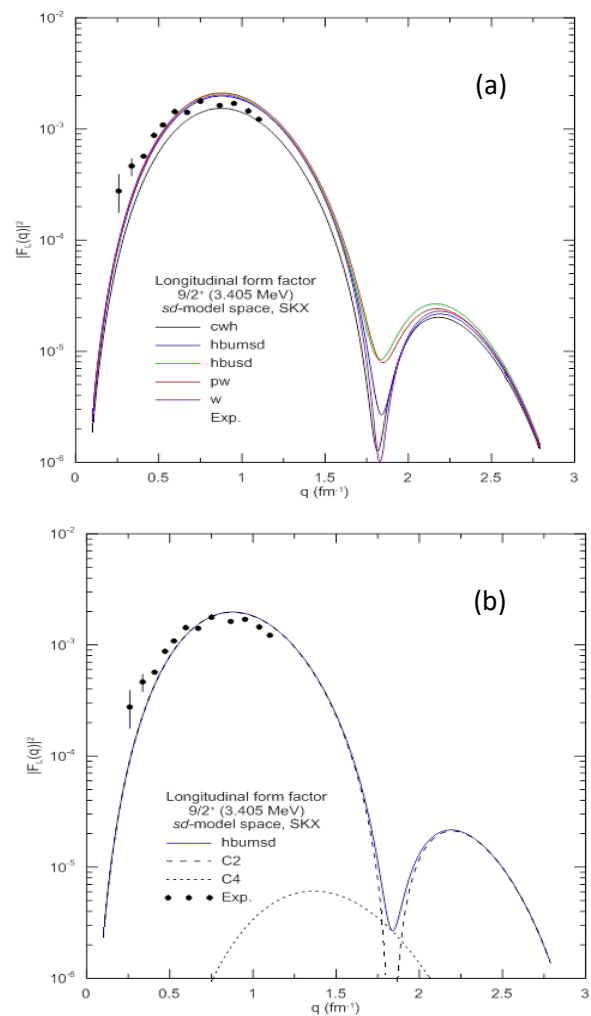
experimental data using SkX parameterization [26]and [18].

In Fig.5 (a) shows the calculated inelastic longitudinal form factors C2 + C4 for the transition $9/2^+$ at (3.405 MeV). Our results are in good agreement with the experimental data of the momentum transfer region (0.3 to 1.25 fm^{-1}) for all five interactions identified especially with the HBUMSD interaction. The contributions of individual C2 and C4 to the long form factor were as seen in Fig.5(b) together with the experimental data to obtain the best interaction. It is seen that the contribution of C4 is negligible, while the contribution of C2 is substantially all in the momentum transfer. The transverse form factors of this transition represented by the sum of the magnetic and electrical form factors for each selected interaction were dissipated in Fig.5 (c). All interactions are in a fine agreement for total transverse form factors. Fig.5 (d) shows the best interaction with the contribution of the electric curve E2+E4 and the magnetic M3+M5 curves. We notice that the contribution of M3+M5 is large, while the contribution of E2+E4 is considered less, Where the contribution is near the region is less than for high momentum transfer (less 0.5 fm-1).
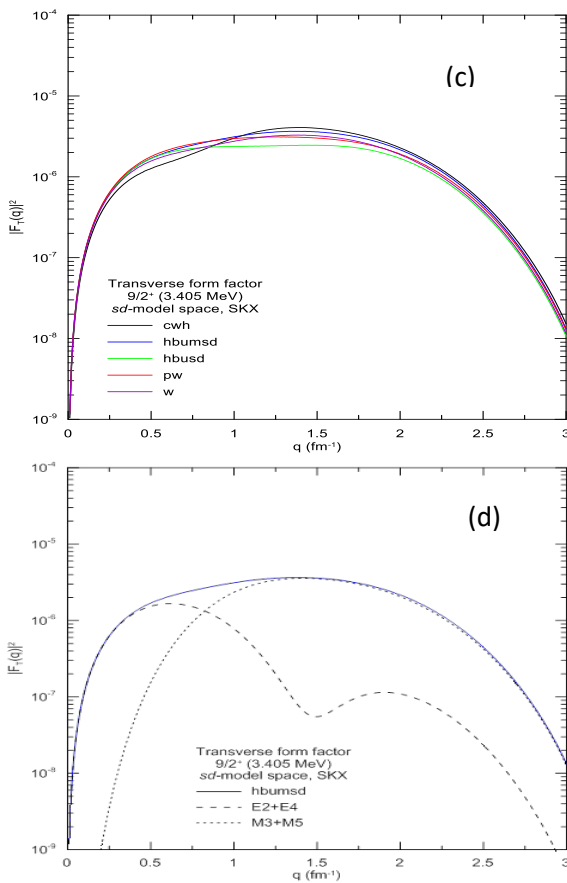

Fig.4 Longitudinal (a and b) and transverse (c and d) form factors in theory, for 7/2+ (1.611 MeV) compared to

Fig.5 Theoretical longitudinal (a and b) and transverse (c and d) form factors for 9/2+ (3.405 MeV) compared to experimental data using SkX parameterization [18, 26].

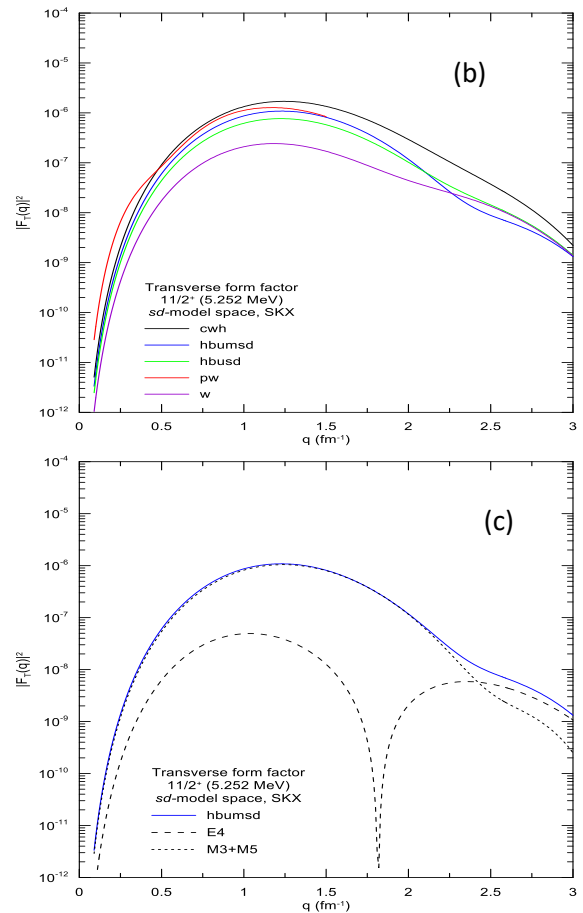Fig.6 Represents the inelastic longitudinal form factors (C2) for $11/2^+$ transition at 5.251 MeV for all interactions. It was found that the theoretical curves agree well with the experimental data. The most compatible interaction for this transition is HBUMSD, with in the momentum transfer (0.9 to 1.2 fm^{-1}). The transverse form factors of this transition represented by the sum of the magnetic and electrical form factors for each selected interaction were dissipated in Fig.6 (b). Fig.6 (c) shows the best interaction with the contribution of the electric curve E4 and the magnetic M3+M5 curves. We notice that the contribution of M3+M5 is large, while the contribution of E4 is considered less.

Fig.6 Theoretical longitudinal and transverse form factors for 11/2+ (a, b, and c), (5.251 MeV) compared to experimental data using SkX parameterization[15].
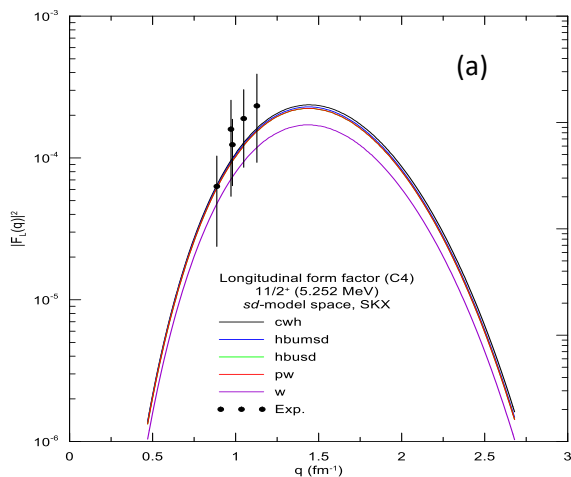
Fig.7 shows a comparison of the experimental energy spectrum and the estimated energy levels for the different interactions identified in this study. That the theoretical and experimental schemes are in agreement has been implemented with great success, one can conclude that reaction W is the most consistent reaction with practical results, followed by reaction of HBUSD. It is obvious that the SkX parameterization of the shell model allows for the prediction of a high density of positive parity states.
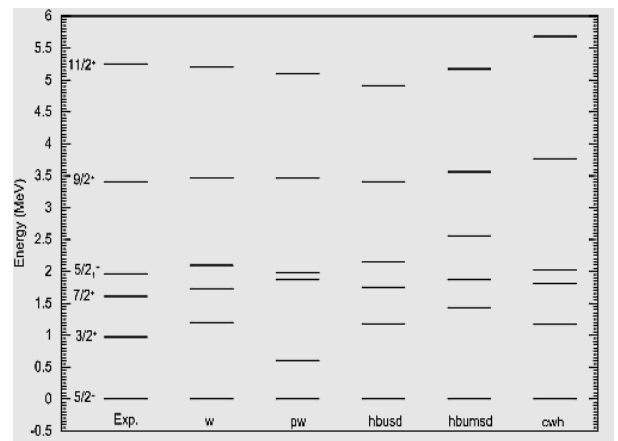

Fig. 7: Comparison of positive parity energy levels of the 25Mg nucleus using different interactions.

The estimated values for all transitions in 25Mg that are considered in this study are tabulated in Table.(1). The agreement is good for the states J= $5/2^+$ and $11/2^+$ and replicated correctly, but there is a little variance for the other states, according to an examination of these values. The B(E2) values are fairly accurate.

Table1: Reduced transition probabilities and excitation energies for the 25Mg nucleus (positive parity states).

$J_i^\pi \to J_f^\pi$	Excitation energy (MeV)		B(E2)(e^2fm^{2J})	
	Theory	Exp.	Theory	Exp.
$5/2^+ \to 1/2^+$		0.585		
$5/2^+ \to 3/2^+$	1.2	0.974		
$5/2^+ \to 7/2^+$	2.095	1.611		
$5/2^+ \to 5/2^+$	1.73	1.964		
$5/2^+ \to 9/2+$	3.464	3.405		
$5/2+ \to 11/2^+$	5.2	5.251		

4 .Conclusions

The structure of the 25Mg nucleus' nuclear nucleus was studied. in this study. For the positive valence states, in the momentum transfer q 0.0 -3.0 fm-1, we calculated the elastic and inelastic electron scattering form factors, as well energy levels and transition probability up to 5.251 MeV excitation energy, were calculated for positive valence states. There has been presented a way for combining Skyrme and shell model computations with positive valence levels. In most situations, the experimental data and the cloned form factors with SKX parameterization match. For studying nuclear composition with the envelope model, the Skyrme interaction has been emphasized as the best and most appropriate method for computing single-segment matrix elements, and it is required for getting a good description of longitudinal and transverse electron scattering form factors.

5. References

[1] R. Longland, C. Iliadis, A. Karakas, Publisher's Note: Reaction rates for the s-process neutron source 22 Ne+ α [Phys. Rev. C 85, 065809 (2012)], Physical Review C, 86 (2012) 019903.

[2] R. Longland, C. Iliadis, G. Rusev, A. Tonchev, R. Deboer, J. Görres, M. Wiescher, Photoexcitation of astrophysically important states in Mg 26, Physical Review C, 80 (2009) 055803.

[3] B. Limata, F. Strieder, A. Formicola, G. Imbriani, M. Junker, H. Becker, D. Bemmerer, A. Best, R. Bonetti, C. Broggini, New experimental study of low-energy (p, γ) resonances in magnesium isotopes, Physical Review C, 82 (2010) 015801.

[4] M. Isaka, M. Kimura, A. Doté, A. Ohnishi, Splitting of the p orbit in triaxially deformed Λ 25 Mg, Physical Review C, 87 (2013) 021304.

[5] M. Isaka, H. Homma, M. Kimura, A. Doté, A. Ohnishi, Modification of triaxial deformation and change of spectrum in Λ 25 Mg caused by the Λ hyperon, Physical Review C, 85 (2012) 034303.

[6] K. Brueckner, Nuclear saturation and two-body forces. II. Tensor forces, Physical Review, 96 (1954) 508.

[7] B. Brown, A. Etchegoyen, W. Rae, NS. Godwin,"code OXBASH (unpublished)", MSU-NSCL Report No, 524 (1985).

[8] E. Caurier, F. Nowacki, Present status of shell model techniques, Acta Physica Polonica B, 30 (1999) 705.

[9] R. Radhi, N. Khalaf, A. Najim, Elastic magnetic electron scattering from 17O, 25Mg and 27Al, Nuclear Physics A, 724 (2003) 333-344.

[10] R. Radhi, A. Hamoudi, K. Jassim, Calculations of longitudinal form factors of p-shell nuclei, using enlarged model space including core-polarization effects with realistic two-body effective interaction, Indian Journal of Physics, 81 (2007) 683-695.

[11] A.A. Al-Sammarraie, F.I. Sharrad, N. Yusof, H.A. Kassim, Longitudinal and transverse electron-nucleus scattering form factors of Mg 25, Physical Review C, 92 (2015) 034327.

[12] A.A. Alzubadi, Shell model and Hartree-Fock calculations of electron scattering form factors for 25Mg nucleus, Iraqi Journal of Physics (IJP), 14 (2016) 28-36.

[13] G.N. Flaiyh, Study of the Static and Dynamic Nuclear Properties and Form Factors for Some Magnesium Isotopes 29-34 Mg, Iraqi Journal of Physics (IJP), 19 (2021) 82-93.

[14] P. Singhal, A. Watt, R. Whitehead, Elastic electron scattering from 23Na, 25Mg and 27Al and a shell-model interpretation, Journal of Physics G: Nuclear Physics, 8 (1982) 1059.

[15] E.W. Lees, C. Curran, T. Drake, W. Gillespie, A. Johnston, R. Singhal, Inelastic electron scattering from 25Mg, Journal of Physics G: Nuclear Physics, 2 (1976) 341.

[16] M. Carvalho, M. Vassanji, D. Rowe, A symplectic model calculation of transverse electron scattering form factors for 24Mg, Physics Letters B, 318 (1993) 273-276.

[17] E. Lees, C. Curran, T. Drake, W. Gillespie, A. Johnston, R. Singhal, Elastic electron scattering from the stable isotopes of magnesium, Journal of Physics G: Nuclear Physics, 2 (1976) 105.

[18] J. Marinelli, J. Moreira, Inelastic transverse electron scattering on Mg 25, Physical Review C, 45 (1992) 1556.

[19] P.B.a.P. Glaudemans, Shell-Model Applications in Nuclear Spectroscopy, , North-Holland, Amsterdam and New York1979.

[20] T. de Forest Jr, J.D. Walecka, Electron scattering and nuclear structure, Advances in Physics, 15 (1966) 1-109.

[21] B. Brown, B. Wildenthal, C. Williamson, F. Rad, S. Kowalski, H. Crannell, J. O'Brien, Shell-model analysis of high-resolution data for elastic and inelastic electron scattering on F 19, Physical Review C, 32 (1985) 1127.

[22] D. Vautherin, D.t. Brink, Hartree-Fock calculations with Skyrme's interaction. I. Spherical nuclei, Physical Review C, 5 (1972) 626.

[23] H. Sagawa, B. Brown, O. Scholten, Shell-model calculations with a Skyrme-type effective interaction, Physics Letters B, 159 (1985) 228-232.

[24] B. Brown, W. Richter, R. Lindsay, Displacement energies with the Skyrme Hartree–Fock method, Physics Letters B, 483 (2000) 49-54.

[25] J. Negele, D. Vautherin, Density-matrix expansion for an effective nuclear hamiltonian, Physical Review C, 5 (1972) 1472.

[26] E. Lees, C. Curran, S. Brian, W. Gillespie, A. Johnston, R. Singhal, The ground state band of 25Mg studied by electron scattering, Journal of Physics G: Nuclear Physics, 1 (1975) L13.

دراسة عوامل التشكل الطولية والمستعرضة الكلية ومساهمات اقطابها في نزاة المغنيسيوم-25 لمستويات التماثل الموجبة بإستخدام تفاعلات مختلفة

نبيل فوزي لطوفي ، سماهر ثابت مشعان

جامعة الانبار ـكلية العلوم ـقسم الفيزياء

الخلاصة:

تم دراسة التركيب النووي لنواة المغنيسيوم- 25 باستخدام نموذج القشرة وتفاعلات سكيرم. لمستويات الطاقة الواطئة ذات التماثل الموجب تم حساب عوامل التشكل للاستطارة الالكترونية الغير مرنة، مستويات الطاقة، كثافة توزيع الشحنة واحتمالات الانتقال. استخدمت معلمـات SKX مـع فضـاء نمـوذج القشـرة sd. افضـل النتائج تم الحصول عليها من تفاعلات HBUMSD,HBUSD,CWH,PW و Wوالتي تم حسابها في فضاء نموذج القشرة sd. طاقـات التهيـج واحتمـالات الانتقـال الى المستوى 2/5+ الارضي تم حسابها ايضا. تم مقارنة نتائج عوامل التشكل ومستويات الطاقة واحتمالات الانتقال مـع البيانـات العمليـة. اوضـحت النتـائج ان نمـوذج القشرة مع تفاعلات سكيرم يمتلك امكانية دراسة التركيب النووي لهذه النواة .